Selective Chromogenic Detection of Thiol-Containing Biomolecules Using Carbonaceous Nanospheres Loaded with Silver Nanoparticles as Carrier

Bo Hu, Yang Zhao, Hai-Zhou Zhu, and Shu-Hong Yu*

Division of Nanomaterials & Chemistry, Hefei National Laboratory for Physical Sciences at Microscale, the School of Chemistry and Materials, University of Science and Technology of China, Hefei 230026, People's Republic of China

ABSTRACT Thiol-containing biomolecules show strong affinity with noble metal nanostructures and could not only stably protect them but also control the self-assembly process of these special nanostructures. A highly selective and sensitive chromogenic detection method has been designed for the low and high molecular weight thiol-containing biomolecules, including cysteine, glutathione, dithiothreitol, and bovine serum albumin, using a new type of carbonaceous nanospheres loaded with silver nanoparticles (Ag NPs) as carrier. This strategy relies upon the place-exchange process between the reporter dyes on the surface of Ag NPs and the thiol groups of thiol-containing biomolecules. The concentration of biomolecules can be determined by monitoring with the fluorescence intensity of reporter dyes dispersed in solution. This new chromogenic assay method could selectively detect these biomolecules in the presence of various other amino acids and monosaccharides and even sensitively detect the thiol-containing biomolecules with different molecular weight, even including proteins.

KEYWORDS: carbonaceous materials · silver nanoparticles · chromogenic detection · thiol-containing biomolecules · protein

In the field of noble metal nanomaterials, thiols have strong affinity with these material surfaces, forming the ultrastable Au−S bonding interactions with gold nanoparticles.[1] A lot of thiol-containing biomolecules, including some aminothiols, peptides, and proteins, have gained much more attention in recent years due to their vital biological functions and important biomarker for diagnosing diseases.[1−4] Thiols could effectively control the growth and self-assembly process of noble metal nanomaterials,[5−9] such as controlling transverse overgrowth of gold nanorods,[5] forming beautiful necklaces by self-assembly of gold nanomaterials,[6] and inducing curvature-directed assembly of gold nanocubes, nanobranches, and nanospheres.[7] In this self-assembly process, due to the unique surface plasmon resonance property of noble metal nanomaterials, with the decreased absorption of the shorter wavelength, as well as the emergency and increased absorption of the longer wavelength.[8,10] Recently, on the basis of this change, some colorimetric,[1,2,11−16] high-performance liquid chromatography (HPLC),[10] and surface-assisted laser desorption/ionization mass spectrometry (SALDI-MS)[17] detection methods have been developed for sensitive and selective detection of low molecular weight thiols, such aminothiols and peptides. Furthermore, Rotello *et al.*[18] have reported that the thiol groups of glutathione could effectively release biomolecules and drug from the surface of gold nanoparticles through the place-exchange reaction both *in vitro* and in cell cultures.

Carbonaceous nanomaterials, as a new and promising biomaterial, have attracted more and more attention because of their high biocompatibility, surface reactivity, chemical stability, and the convenient "green" preparation method.[19−22] A large number of surface functional groups of carbonaceous materials make it easy to link biomolecules or drugs[23,24] and load with noble metal nanoparticles.[17,25,26]

Here, we report a new chromogenic detection method for the selective and sensitive detection of thiol-containing biomolecules, based on the strong effect of surface thiol groups and silver nanoparticles (Ag NPs) as well as the effective carrier of carbonaceous nanospheres C(NPs) loaded with Ag NPs. Our strategy was to load the reporter dyes (fluorescein isothiocyanate (FITC)) on the surface of hybrid spheres that were accessible to exchange by thiol groups of thiol-containing biomolecules. First, FITC@Ag NPs@C NPs hybrid spheres were used as reporter materials, which were synthesized by first decoration of Ag NPs on the C NPs and the following modification of

* Address correspondence to shyu@ustc.edu.cn.

Received for review January 25, 2011 and accepted March 10, 2011.

Published online March 10, 2011
10.1021/nn2003053

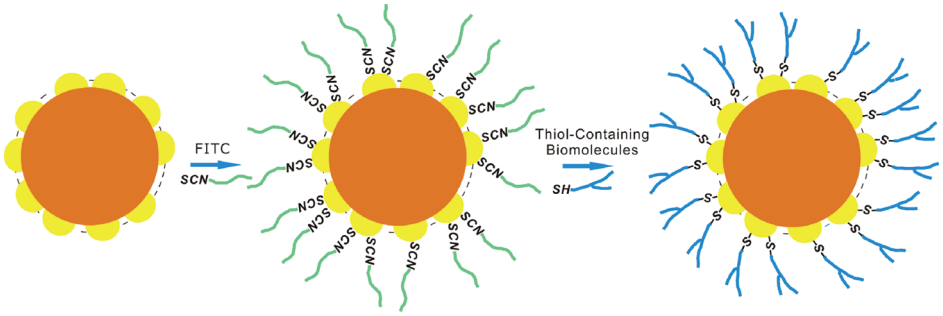

Scheme 1. Schematic illustration of thiol-containing biomolecule detection based on the FITC@Ag NPs@C NPs hybrid spheres. First, hybrid materials were synthesized by first decoration of Ag NPs on the carbonaceous nanospheres and following modification of FITC on the surface of hybrids. Then, thiol groups of biomolecules place-exchanged FITC molecules, and the fluorescence signal for exchange was governed by the photoemission property of FITC in the solution.

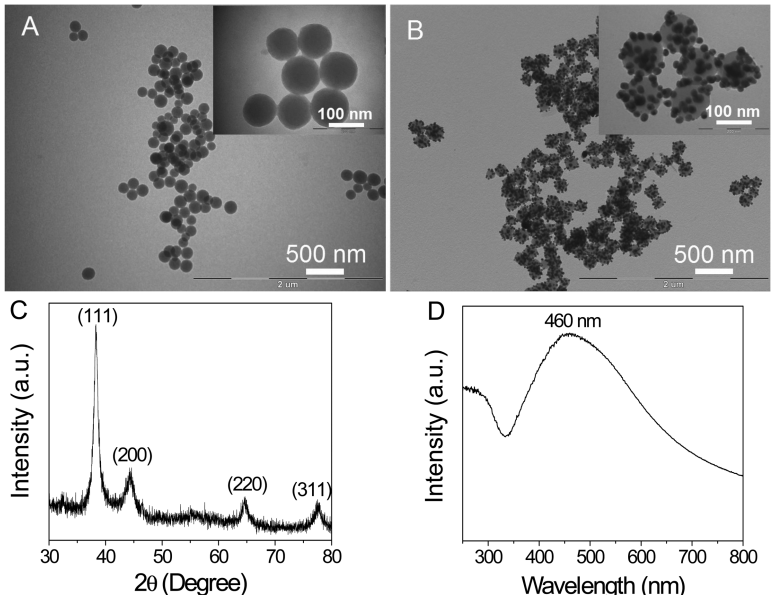

Figure 1. (A) TEM image of carbonaceous nanospheres (C NPs). Inset shows the magnified TEM image. (B) TEM image of silver nanoparticle (Ag NPs)-modified C NPs hybrid spheres (Ag NPs@C NPs). Inset shows the magnified TEM image. (C) XRD pattern of the Ag NPs@C NPs hybrid spheres. (D) UV−vis absorption spectrum of the Ag NPs@C NPs hybrid materials.

FITC molecules on the surface of Ag NPs (Scheme 1). Second, the fluorescence signal for exchange was governed by the photoemission property of FITC in the solution, which depended on the exchange process between FITC and thiol groups (Scheme 1). We chose FITC as reporter dye because, while FITC modified Ag NPs with the S═C═N− groups, it could be just effectively exchanged by thiol groups, but not other groups, including hydroxyl, aldehyde, carboxyl, and amino groups. C NPs, with high surface functional groups, such as hydroxyl, aldehyde, and carboxyl groups,[19,20] could greatly increase the capacity of the reduced Ag NPs and the dispersion ability in the buffer solution.

RESULTS AND DISCUSSION

The synthesis of FITC@Ag NPs@C NPs hybrid materials has some beneficial effects: (1) C NPs produced by a hydrothermal carbonization process exhibited excellent surface reactivity and can *in situ* reduce silver ions without the addition of any reducing agent.[21] The produced Ag NPs@C NPs were very stable. FITC molecules could be prone to modify their surface without the influence of other surfactants. (2) The high surface reactivity could greatly increase the amount of Ag NPs on the surface of C NPs.[17] FITC molecules were prone to noncovalently adsorb on the surface of Ag NPs but not the surface of C NPs because C NPs have the same negative surface potential with FITC molecules. So the more Ag NPs, the more FITC adsorbed. (3) The synthesized FITC@Ag NPs@C NPs hybrid spheres have shown great dispersion ability in the sodium acetate buffer solution (pH 4.8−5.8) and could effectively react with the thiol groups of biomolecules in the solution. (4) The whole synthesis process was more convenient, mild, and repeatable, as well as low cost.

A representative transmission electron microscope (TEM) image of C NPs is shown in Figure 1A, indicating that the produced nanoparticles are spherical and have an average diameter around 100 nm. Figure 1B shows the typical TEM image of the Ag NPs@C NPs hybrid spheres. Some individual Ag NPs, with an average diameter of around 15 nm, were decorated on the surface of C NPs. The X-ray diffraction (XRD) pattern of the hybrid spheres (Figure 1C) shows a face-centered cubic silver crystal structure (JCPDS card No. 04−0783). The UV−vis absorption spectra of the Ag NPs@C NPs hybrid materials showed the surface plasmon response band centered at 460 nm (Figure 1D). Compared with the surface plasmon response of individual Ag NPs,[27] this red shift was attributed to interparticle plasmon coupling between the amounts of the surface-modified Ag NPs.[9,23,26,28]

To determine the selectivity of this assay, we studied its chromogenic response to the other amino acids or monosaccharide, at a concentration of 10 μM and the pH value of a sodium acetate buffer solution of 5.0 (Figure 2). The fluorescence intensity of the solution in the presence of these amino acids and monosaccharides remained unchanged. The main reason is that the amino and carboxyl groups in amino acids as well as the hydroxyl and aldehyde groups in the monosaccharides could not effectively place-exchange FITC molecules on the surface of Ag NPs. It is clear that cysteine has shown a significantly higher fluorescence ratio (F/F_0), indicating that the thiol functionality in cysteine is essential for spectral changes.

The sensitivity and quantification of this chromogenic assay toward typical thiol-containing biomolecules have been carefully studied. We chose four typical thiol-containing biomolecules for this method, including the amino acids of cysteine, the peptide of glutathione, the protein of bovine serum albumin (BSA) and the small biomolecule of dithiothreitol. These biomolecules were analyzed at different pH values of the sodium acetate buffer solution, which is equal or very close to their isoelectric points. Figure 3 shows the fluorescence ratio (F/F_0) profiles of this method against different concentrations of biomolecules. It can be seen that the fluorescence ratio increases with increasing biomolecule concentration. We could find the satisfied detection scopes from each of these biomolecules. Four representative plots are presented in Figure 3, and each of them exhibits good linearity ($R^2 > 0.98$). The linear detection range for BSA, cysteine, glutathione, and dithiothreitol are 20−500 μg/mL, 0.2−10 μM, 0.02−1 μM, and 0.02−1 μM, respectively. The limits of detection for BSA, cysteine, glutathione, and dithiothreitol are 20 μg/mL, 0.2 μM, 20 nM, and 20 nM, respectively. To the best of our knowledge, the detection limit achieved with this chromogenic method represented the same magnitude with the lowest detection limit of the common colorimetric method,[14] especially for glutathione and dithiothreitol.

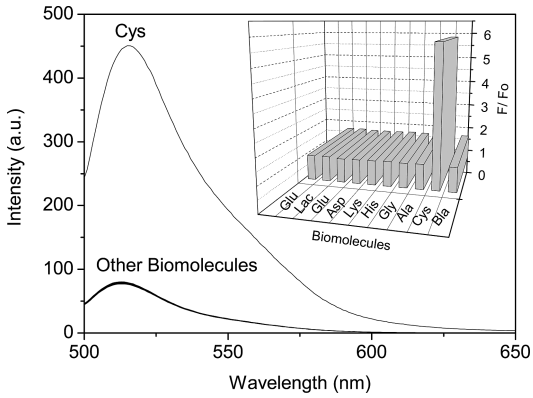

Figure 2. Differences of the fluorescence intensity of the chromogenic detection system in the presence of cysteine and other amino acids and monosaccharides under the concentration of 10 μM and the pH value of the sodium acetate buffer solution of 5.0, including blank experiment (Bla), glucose (Glu), lactose (Lac), glutamic acid (Glu), aspartic acid (Asp), lysine (Lys), histidine (His), glycine (Gly), alanine (Ala), cysteine (Cys). The inset image is the 3D plot showing the selectivity of cysteine, other amino acids, and monosaccharides.

Interestingly, as shown in Figure 3, this chromogenic detection method could sensitively determine the low molecular weight thiols (cysteine, glutathione, and dithiothreitol) and also the high molecular weight thiol (BSA). However, in the colorimetric detection method,[2,6,10,11,13,14] only the low molecular weight thiols could effectively place-exchange and self-assemble noble metal nanostructures, forming the obvious change of the color and absorption spectra. Proteins, due to their large size, complex structure, and great coulombic repulsion,[29] could ineffectively aggregate these nanostructures and give obvious changes.[1] In our new chromogenic competition assay, there are two beneficial effects for the effective determination of protein. First, it has been known that several protein molecules could absorb on the noble metal nanostructures.[30−32] Consequently, BSA could place-exchange FITC molecules on the surface of Ag NPs, especially, using the bare thiol group. Our experimental results have effectively demonstrated this place-exchange process of BSA. Second, our chromogenic method has no use for the self-assembly of noble metal nanostructures, providing obvious changes of the color and absorption spectra. We just need to measure the solution fluorescence intensity of FITC molecules that were place-exchanged by the BSA from the FITC@Ag NPs @C NPs hybrid spheres. Furthermore, it is interesting to find that this assay could selectively detect thiol-containing proteins (Figure 4). Collagen, without

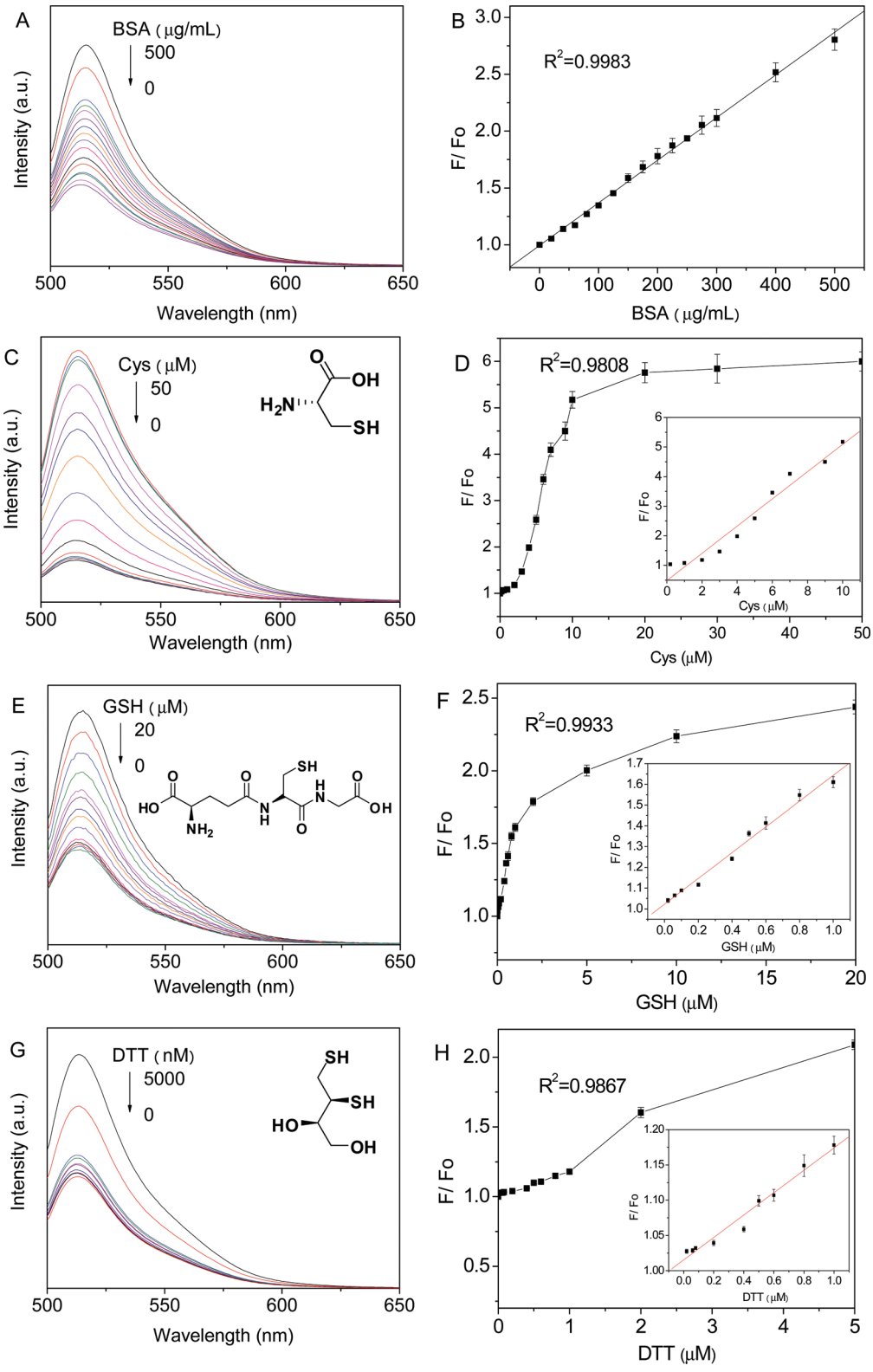

Figure 3. Fluorescence spectra of this chromogenic assay upon addition of different concentrations of BSA (A), cysteine (C), glutathione (E), and dithiothreitol (G). Linear plots of F/F_0 as a function of biomolecular concentrations of BSA (B), cysteine (D), glutathione (F), and dithiothreitol (H).

including the amino acids part of cysteine, could not effectively place-exchange FITC molecules on the surface of Ag NPs. However, because of the high molecular weight and complex structures, different thiol-containing proteins have also shown different place-exchange ability for the FITC molecules.

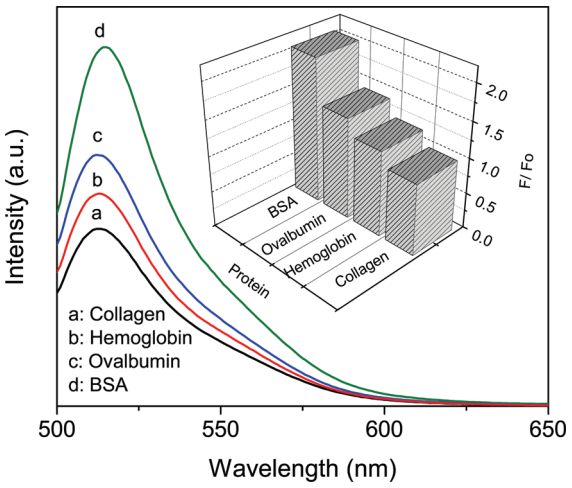

Figure 4. Fluorescence spectra of this chromogenic assay upon addition of different proteins under the concentration of 300 μg/mL and the pH values of the sodium acetate buffer solution of collagen (5.0), hemoglobin (7.0), ovalbumin (4.8), and BSA (4.8). The inset image is the 3D plot showing the different activity of proteins, including BSA, ovalbumin, hemoglobin, and collagen.

CONCLUSION

In conclusion, we have demonstrated a selective, sensitive, and quantified chromogenic detection method for thiol-containing biomolecules based on the strong effect of surface thiol groups and Ag NPs which are loaded on highly active carbonaceous nanospheres. The high degree of discrimination in this assay may be mainly attributed to two features: (1) FITC molecules were stably adsorbed on the surface of Ag NPs located on carbonaceous nanospheres, which results in the selective detection of the thiol-containing biomolecules in the presence of various other amino acids and monosaccharides; (2) as in the fluorescence analysis, the chromogenic signal depends on the place-exchanged FITC molecules in the solution, but not the aggregation of the noble metal nanostructures, which leads to the sensitive detection of high molecular weight thiols, even thiol-containing proteins. The present study opens up a new possibility for the rapid, facile, selective, and reliable diagnosis of thiol-containing biomolecules and biologically important molecular systems containing thiol groups.

MATERIALS AND METHODS

All reagents are of analytical grade and used without further purification.

Synthesis of Carbonaceous Nanospheres. Carbonaceous nanospheres were prepared according to the literature with some slight modifications.[21] Briefly, 8 g of glucose was dissolved in 80 mL of deionized water with stirring. After forming the clear solution, the solution was transferred into a Teflon-lined autoclave of 100 mL and heated to 180 °C and kept at that temperature for 8 h. After cooling to room temperature, a solution with brown color was obtained. The product was centrifuged and washed several times by deionized water and pure ethanol to remove other impurities and finally freeze-dried in a vacuum.

Synthesis of Ag NPs@C NPs Hybrid Spheres. Ten milligrams of the produced carbonaceous nanospheres and 100 mL of deionized water were added to a 250 mL flask. The solution was ultrasonically pretreated for 5 min, then 100 mg of $AgNO_3$ was added. The mixed solutions were refluxed at 100 °C in an oil bath for 2 h. The products were centrifuged and washed several times by deionized water to remove excess $AgNO_3$ and finally freeze-dried in a vacuum.

Synthesis of FITC@Ag NPs@C NPs Hybrid Spheres. A 50 mL FITC ethanol solution (1 mM) was mixed with 50 mL of Ag NPs@C NPs hybrid material aqueous solution (1 mg/mL), and the mixture was kept at 37 °C for 1 h. The product was centrifuged and washed several times with deionized water to remove excess FITC and finally freeze-dried in a vacuum.

Characterization. X-ray powder diffraction patterns (XRD) of the product were obtained on a Japan Rigaku DMax-γA rotation anode X-ray diffractometer equipped with graphite monochromatized Cu Kα radiation (λ = 1.54178 Å). Transmission electron microscope (TEM) photographs were taken on a Hitachi model H-800 transmission electron microscope at an accelerating voltage of 200 kV. UV−vis spectra were recorded with a ShimadzuUV-240 spectrophotometer at room temperature. Photoluminescence emission was obtained at room temperature with a Hitachi F-7000 fluorescence spectrometer.

Determination of Thiols. In a typical process, 1 mL of FITC@Ag NPs@C NPs hybrid material aqueous solution (1 mg/mL) was added to the sodium acetate buffer solution, then 500 μL of different concentrations of thiol solutions was added. The mixtures were constant to 25 mL using the sodium acetate buffer solution. Then, the mixtures were gently shook and left at room temperature for 30 min. After that, the mixtures were centrifuged and the above clear solution was measured for PL spectra. In this process, different pH values of the sodium acetate buffer solutions were, for cysteine (Cys), glutathione (Glu), bovine serum albumin (BSA), and dithiothreitol (DTT), 5.0, 5.8, 4.8, and 5.2, respectively.

Acknowledgment. S.H.Y. acknowledges the funding support from the National Basic Research Program of China

(2010CB934700), the National Natural Science Foundation of China (Nos. 91022032, 50732006), and International Science & Technology Cooperation Program of China (2010DFA41170).

REFERENCES AND NOTES

1. Chen, S. J.; Chang, H. T. Nile Red-Adsorbed Gold Nanoparticles for Selective Determination of Thiols Based on Energy Transfer and Aggregation. *Anal. Chem.* **2004,** *76*, 3727–3734.
2. Sudeep, P. K.; Joseph, S. T. S.; Thomas, K. G. Selective Detection of Cysteine and Glutathione Using Gold Nanorods. *J. Am. Chem. Soc.* **2005,** *127*, 6516–6517.
3. Ivanov, A. R.; Nazimov, I. V.; Baratova, L. Determination of Biologically Active Low-Molecular-Mass Thiols in Human Blood I. Fast Qualitative and Quantitative, Gradient and Isocratic Reversed-Phase High-Performance Liquid Chromatography with Photometric and Fluorescence Detection. *J. Chromatogr. A* **2000,** *895*, 157–166.
4. Ivanov, A. R.; Nazimov, I. V.; Baratova, L. A. Determination of Biologically Active Low-Molecular-Mass Thiols in Human Blood II. High-Performance Capillary Electrophoresis with Photometric Detection. *J. Chromatogr. A* **2000,** *895*, 167–171.
5. Kou, X. S.; Zhang, S. Z.; Yang, Z.; Tsung, C. K.; Stucky, G. D.; Sun, L. D.; Wang, J. F.; Yan, C. H. Glutathione- and Cysteine-Induced Transverse Overgrowth on Gold Nanorods. *J. Am. Chem. Soc.* **2007,** *129*, 6402–6404.
6. Zhang, S. Z.; Kou, X. S.; Yang, Z.; Shi, Q. H.; Stucky, G. D.; Sun, L. D.; Wang, J. F.; Yan, C. H. Nanonecklaces Assembled from Gold Rods, Spheres, and Bipyramids. *Chem. Commun.* **2007,** 1816–1818.
7. Kou, X. S.; Sun, Z. H.; Yang, Z.; Chen, H. J.; Wang, J. F. Curvature-Directed Assembly of Gold Nanocubes, Nanobranches, and Nanospheres. *Langmuir* **2009,** *25*, 1692–1698.
8. Lim, I. I. S.; Mott, D.; Ip, W.; Njoki, P. N.; Pan, Y.; Zhou, S. Q.; Zhong, C. J. Interparticle Interactions in Glutathione Mediated Assembly of Gold Nanoparticles. *Langmuir* **2008,** *24*, 8857–8863.
9. Guarise, C.; Pasquato, L.; Scrimin, P. Reversible Aggregation/Deaggregation of Gold Nanoparticles Induced by a Cleavable Dithiol Linker. *Langmuir* **2005,** *21*, 5537–5541.
10. Lu, C.; Zu, Y. B.; Yam, V. W. W. Specific Postcolumn Detection Method for HPLC Assay of Homocysteine Based on Aggregation of Fluorosurfactant-Capped Gold Nanoparticles. *Anal. Chem.* **2007,** *79*, 666–672.
11. Durocher, S.; Rezaee, A.; Hamm, C.; Rangan, C.; Mittler, S.; Mutus, B. Disulfide-Linked, Gold Nanoparticle Based Reagent for Detecting Small Molecular Weight Thiols. *J. Am. Chem. Soc.* **2009,** *131*, 2475–2477.
12. Zhang, F. X.; Han, L.; Israel, L. B.; Daras, J. G.; Maye, M. M.; Ly, N. K.; Zhong, C. J. Colorimetric Detection of Thiol-Containing Amino Acids Using Gold Nanoparticles. *Analyst* **2002,** *127*, 462–465.
13. Lu, C.; Zu, Y. B. Specific Detection of Cysteine and Homocysteine: Recognizing One-Methylene Difference Using Fluorosurfactant-Capped Gold Nanoparticles. *Chem. Commun.* **2007,** 3871–3873.
14. Li, L.; Li, B. X. Sensitive and Selective Detection of Cysteine Using Gold Nanoparticles as Colorimetric Probes. *Analyst* **2009,** *134*, 1361–1365.
15. Lee, J. S.; Ulmann, P. A.; Han, M. S.; Mirkin, C. A. A DNA−Gold Nanoparticle-Based Colorimetric Competition Assay for the Detection of Cysteine. *Nano Lett.* **2008,** *8*, 529–533.
16. Elghanian, R.; Storhoff, J. J.; Mucic, R. C.; Letsinger, R. L.; Mirkin, C. A. Selective Colorimetric Detection of Polynucleotides Based on the Distance-Dependent Optical Properties of Gold Nanoparticles. *Science* **1997,** *277*, 1078–1081.
17. Qian, H. S.; Antonietti, M.; Yu, S. H. Hybrid "Golden Fleece": Synthesis and Catalytic Performance of Uniform Carbon Nanoribers and Silica Nanotubes Embedded with a High Population of Noble-Metal Nanoparticles. *Adv. Funct. Mater.* **2007,** *17*, 637–643.
18. Hong, R.; Han, G.; Fernandez, J. M.; Kim, B. J.; Forbes, N. S.; Rotello, V. M. Glutathione-Mediated Delivery and Release Using Monolayer Protected Nanoparticle Carriers. *J. Am. Chem. Soc.* **2006,** *128*, 1078–1079.
19. Hu, B.; Yu, S. H.; Wang, K.; Liu, L.; Xu, X. W. Functional Carbonaceous Materials from Hydrothermal Carbonization of Biomass: An Effective Chemical Process. *Dalton Trans.* **2008,** 5414–5423.
20. Hu, B.; Wang, K.; Wu, L. H.; Yu, S. H.; Antonietti, M.; Titirici, M. M. Engineering Carbon Materials from the Hydrothermal Carbonization Process of Biomass. *Adv. Mater.* **2010,** *22*, 813–828.
21. Sun, X. M.; Li, Y. D. Colloidal Carbon Spheres and Their Core/Shell Structures with Noble-Metal Nanoparticles. *Angew. Chem., Int. Ed.* **2004,** *43*, 597–601.
22. Wang, Q.; Li, H.; Chen, L. Q.; Huang, X. J. Monodispersed Hard Carbon Spherules with Uniform Nanopores. *Carbon* **2001,** *39*, 2211–2214.
23. Cui, R. J.; Liu, C.; Shen, J. M.; Gao, D.; Zhu, J. J.; Chen, H. Y. Gold Nanoparticle-Colloidal Carbon Nanosphere Hybrid Material: Preparation, Characterization, and Application for an Amplified Electrochemical Immunoassay. *Adv. Funct. Mater.* **2008,** *18*, 2197–2204.
24. Selvi, B. R.; Jagadeesan, D.; Suma, B. S.; Nagashankar, G.; Arif, M.; Balasubramanyam, K.; Eswaramoorthy, M.; Kundu, T. K. Intrinsically Fluorescent Carbon Nanospheres as a Nuclear Targeting Vector: Delivery of Membrane-Impermeable Molecule To Modulate Gene Expression *In Vivo*. *Nano Lett.* **2008,** *8*, 3182–3188.
25. Yu, S. H.; Cui, X. J.; Li, L. L.; Li, K.; Yu, B.; Antonietti, M.; Colfen, H. From Starch to Metal/Carbon Hybrid Nanostructures: Hydrothermal Metal-Catalyzed Carbonization. *Adv. Mater.* **2004,** *16*, 1636–1640.
26. Tang, S. C.; Vongehr, S.; Meng, X. K. Carbon Spheres with Controllable Silver Nanoparticle Doping. *J. Phys. Chem. C* **2010,** *114*, 977–982.
27. Hu, B.; Wang, S. B.; Wang, K.; Zhang, M.; Yu, S. H. Microwave-Assisted Rapid Facile "Green" Synthesis of Uniform Silver Nanoparticles: Self-Assembly into Multilayered Films and Their Optical Properties. *J. Phys. Chem. C* **2008,** *112*, 11169–11174.
28. Thomas, K. G.; Barazzouk, S.; Ipe, B. I.; Joseph, S. T. S.; Kamat, P. V. Uniaxial Plasmon Coupling through Longitudinal Self-Assembly of Gold Nanorods. *J. Phys. Chem. B* **2004,** *108*, 13066–13068.
29. Huang, Y. F.; Huang, C. C.; Chang, H. T. Exploring the Activity and Specificity of Gold Nanoparticle-Bound Trypsin by Capillary Electrophoresis with Laser-Induced Fluorescence Detection. *Langmuir* **2003,** *19*, 7498–7502.
30. Gole, A.; Dash, C.; Ramakrishnan, V.; Sainkar, S. R.; Mandale, A. B.; Rao, M.; Sastry, M. Pepsin−Gold Colloid Conjugates: Preparation, Characterization, and Enzymatic Activity. *Langmuir* **2001,** *17*, 1674–1679.
31. Cobbe, S.; Connolly, S.; Ryan, D.; Nagle, L.; Eritja, R.; Fitzmaurice, D. DNA-Controlled Assembly of Protein-Modified Gold Nanocrystals. *J. Phys. Chem. B* **2003,** *107*, 470–477.
32. Bertsch, M.; Mayburd, A. L.; Kassner, R. J. The Identification of Hydrophobic Sites on the Surface of Proteins Using Absorption Difference Spectroscopy of Bromophenol Blue. *Anal. Biochem.* **2003,** *313*, 187–195.